Tissue Engineering and Regenerative Medicine

A novel filtration system for point of care washing of cellular therapy products

Journal:	*Journal of Tissue Engineering and Regenerative Medicine*
Manuscript ID	TERM-16-0050.R1
Wiley - Manuscript type:	Research Article
Date Submitted by the Author:	n/a
Complete List of Authors:	Tostoes, Rui; University College London, Biochemical Engineering Dodgson, John; Dodgson Associates LTD Weil, Benjamin; University College London, Biochemical Engineering Gerontas, Spyridon; University College London, Biochemical Engineering Mason, Chris; University College London, Department of Biochemical Engineering Veraitch, Farlan; University College London, Biochemical Engineering
Keywords:	filtration, cell therapy, cell processing, stem cell processing, cell washing, point of care, cell manufacturing, cell delivery

A novel filtration system for point of care washing of cellular therapy products

Rui Tostoes[1], John R. Dodgson[2], Ben Weil[1], Spyridon Gerontas[1], Chris Mason[1], Farlan Veraitch[1]

1 – The Advanced Centre for Biochemical Engineering, Department of Biochemical Engineering, University College London, Bernard Katz Building, Gower Street, London WC1H 0AH, UK

2 – Dodgson Associates Ltd., London, UK

Abstract

The cell therapy industry would greatly benefit from a simple point of care solution to remove Dimethyl Sulfoxide (DMSO) from small volume thawed cell suspensions prior to injection. We have designed and validated a novel dead-end filtration device, which takes advantage of the higher density of thawed cell suspensions to remove the DMSO and protein impurities from the cell suspension without fouling the filter membrane. The filter was designed to avoid fluid circuits and minimize the surface area that is contacted by the cell suspension, thus reducing cell losses by design.

The filtration process was established through optimization of the fluid flow configuration, backflush cycles and filter geometry. Overall, this novel filtration device allows for a 1 mL of thawed cryopreserved cell suspensions, containing 10^7 cells of a foetal lung fibroblast cell line (MRC-5), to be washed in less than 30 minutes. More than 95% of the DMSO and up to 94% of the Albumin-Fluorescein-Isothiocyanate content can be removed while the viable cell recovery is higher than 80%. We have also demonstrated that this system can be used for bone marrow-derived human mesenchymal stem cells with more than 73% cell recovery and 85% DMSO reduction. This is the first time that a dead end (normal) filtration process has been used to successfully wash high density human cell suspensions. In practice, this novel solid-liquid separation technology fills the need for small volume washing in closed processing systems for cellular therapies.

1. Introduction

The cryopreservation of cellular therapy products is usually performed by controlled-rate freezing (1-5°C/min) in the presence of DMSO, which is the prefered cryopreservation agent (CPA) in virtually every cryopreservation solution (Rowley 2009). This is due to its efficient diffusion across the cell membrane coupled with the ability to prevent intracellular ice formation and osmotic stress during slow rate freezing (Mazur 1984). In the treatment of blood disorders the cell product may be infused to patients without any reduction in DMSO concentration even though the presence of this CPA has been shown to cause nausea, vomiting, cardiac arrhythmia (Cox et al. 2012) and, less frequently, more severe adverse reactions such as neurotoxicity (Abdelkefi et al. 2009), cardiac arrest or epileptic seizure (Cox et al. 2012). Thus, safety concerns are raised when the cellular product consists of a small volume (<10 mL) cell suspension which will be injected into a solid tissue such as the brain or heart (FDA 1997). Such an injection is likely to expose the patient's cells to a much higher DMSO concentration than a blood stream infused product. Although there is no safety data for concentrated DMSO injections in humans, there is published work in animals (Galvao et al. 2014) and brain tissue culture (Tamagnini et al. 2014). These data strongly suggest that a reduction in DMSO concentration is required for cell therapies which are administered via injection into solid tissues and should be performed even in infused cell therapies.

To reduce the DMSO concentration in thawed cell suspensions the most common process is open lab centrifugation. This process is only acceptable in a laminar flow chamber placed in a grade B cleanroom background, which represents an unacceptable financial burden for the current Point of Care (POC) sites such as hospitals or clinics that do not have a cell-processing facility. Another solution is the use of closed centrifugal systems such as the COBE 2991 (Terumo BCT, Colorado, USA) or Sepax S-100 devices (Biosafe S.A., Eysins, Switzerland). These can be used to separate mononuclear cells from red blood cells or as cell washing devices, reaching 97% removal of the DMSO content (Rodríguez et al. 2004) and a total nucleated cell recovery of 75% in cryopreserved peripheral blood progenitor cell products for autologous infusion (Sánchez-Salinas et al. 2012). While these centrifuge-based systems are efficient, they are expensive and not amenable to small scale cell

processing. Hanna and colleagues have described a microfluidic device which removes up to 70% of the initial DMSO concentration from fresh cell suspensions spiked with the cryoprotectant in a three-stream diffusion system (Hanna et al. 2012). The post-wash viable cell recovery reported by these authors was above 95%. Recently, a dilution-filtration system has been reported by Zhou *et al*. This system relies on a tangential flow filtration system (TFF) which enables the removal of 93% of the CPA (glycerol in this instance) from thawed human red blood cells with a viable cell recovery of 91% (Zhou et al. 2011). The main disadvantage of TFF based methods is that they are mostly used for volumes starting at hundreds of mL or litres, and any scale down design of a TFF will include an external circuit where cells are likely to be lost either by liquid adsorption to the material or shear (Jaouen et al. 1999; Kuo et al. 2010). Overall, there is an unmet need for a small scale solid-liquid separation technologies which are cost-effective, simple to operate and enable a high cell recovery.

In this work, we have designed and validated a novel dead end filtration device for the removal of DMSO from 1 mL thawed cell suspensions. A typical dead-end filtration operation produces an exponential pressure increase in the retentate chamber due to the progressive membrane clogging by the retained cells (Rushton et al. 2000; Xu and Chellam 2005). However, it is also a simple system with no moving parts and thus amenable to become a cost-efficient closed point of care solution for cell washing. The location of the filter membrane on top of the cell suspension and the non-turbulent flow allowed the thawed cell suspension to form a bed at the bottom of the filter device and limit the contact of the cells with the filter membrane, thus enabling the dead end filtration to progress for long enough to remove more than 95% of the DMSO. This device was also designed to have a minimal contact area with cells, to avoid cell losses due to liquid adsorption into long fluidic circuits. With this minimal surface area approach the viable cell recoveries were above 80%, after the filtration of thawed 1mL cell suspensions.

2. Materials and Methods

2.1. Cell culture and cryopreservation

The human lung fibroblast cell line MRC-5 (ATCC Catalog No. CCL-171) was used as a model cell line throughout this work. These cells were cultured for a maximum of 40 population doublings (PD) as these cells can reach 42 PD without senescence, according to the supplier. The cells were cultured

in Eagle's Minimum Essential Medium (EMEM, M5650 Sigma-Aldrich UK) supplemented with 10% Foetal Bovine Serum (FBS, Seralab UK), 1% Glutamine and 1% MEM Non-Essential Amino Acids (NEAA, GIBCO, UK) using Nunc T-flasks with 175 cm^2 surface area (Thermo Scientific, UK). Bone Marrow-derived human Mesenchymal Stromal Cells (hMSC) from 2 different donors were purchased from Lonza (Poietics™ human mesenchymal stem cells) and cultured in complete growth medium: DMEM low glucose (21885-025, Life Technologies, UK) supplemented with 10% FBS, 1% NEAA and 1 ng/mL recombinant human basic Fibroblast Growth Factor (bFGF, R&D Systems, MN, US). The hMSCs were cultured for expansion up to passage 7, to minimize the senescence of the population and used as a cell therapy-relevant model to validate the filtration system developed in this work. The hMSC were differentiated using GIBCO® StemPro reagents (GIBCO,UK): For adipogenic, chondrogenic and osteogenic differentiation, hMSCs were seeded into 12-well plates at 1 x 10^4 cells/cm^2, 1.6 x 10^7 cells/mL 10 µL droplets and 5 x 10^3 cells/cm^2, respectively. After 24h in culture in complete growth medium, the media was discarded and 1 ml of Adipogenesis, Chondrogenesis or Osteogenesis Differentiation Medium (StemPro Differentiaiton Kit, GIBCO, Invitrogen) were added to each well. Medium was fully exchanged every 3 days and at day 21 cells were washed in 1X PBS and fixed at room temperature, with 4% paraformaldehyde (PFA), for 10 minutes for adipogenesis cultures and 30 minutes for chondrogenesis and osteogenesis cultures. For adipogenesis cultures, 60% isopropanol was added to the cells and let sit for 5 minutes. Cells were then stained with a filtered solution of 0.3% w/v Oil Red O/isopropanol in distilled water 3:2 for 5 minutes, rinsed under tap and counterstained with hematoxilin for 1 minute. For chondrogenesis cultures, 1% Alcian Blue solution prepared in 0.1M HCl was used to stain the chondrocytes. After 30 minutes, cells were rinsed twice in 0.1M HCL and then under running tap water. For osteogenesis, . 2% Alizarin Red S solution (pH 4.2) was added for 5 minutes and then the wells were carefully rinsed with distilled water to avoid the micromasses disruption.

For cryopreservation, cells were exposed to Trypsin (Sigma-Aldrich, UK) for 5 min at 37 °C and the reaction was stopped by adding 2 volumes of EMEM (supplemented with 10% FBS) per volume of trypsin. The resulting cell suspension was centrifuged at 300*g* for 5 min at room temperature, washed with PBS and centrifuged again under the same conditions. The washed cell pellet was resuspended in

cold (2-8 °C) CryoStor™ containing 5% v/v of DMSO (CS5, BioLife Solutions, WA, USA) to yield 1 mL single cell suspension containing 10-20 million cells/mL. This cell suspension was dispensed into 3 mL Crystal™ vials (Aseptic Technologies, Belgium), incubated for 10 minutes on ice and then transferred to a -80 °C freezer where it was cooled at an approximate rate of -1 °C/min, using a CoolCell container (BioCision, CA, US) and kept up to a maximum of 1 month before use.

2.2. Device design and operation

The filter devices were designed using AutoCad 2011 (Autodesk, CA 94903, USA) and manufactured by machining in UCL's Biochemical Engineering workshop, using either Poly(methyl methacrylate) (PMMA) or Stainless Steel 316 (SS) as a the base material, and by injection molding using the Protomold service from Protolabs, UK. The base material used for injection molding was Cyclic Olefin Co-polymer (COC).

All the devices were designed to allow the 1 mL thawed cell suspension to form an undisturbed bed while the washing buffer flowed through the cell suspension. This configuration minimized and delayed the progressive filter clogging typical in a dead end filtration process. The design shown in Figure 1A enabled the formation of this cell bed by localizing the filter membrane above the cell suspension and ensuring that the lower chamber had a higher volume than that same loaded cell suspension, such that during the wash operation there was a decreasing cell concentration from the top surface of the cell bed to the filter membrane (Figure 1B, top). The wash step was performed by flowing wash buffer (PBS) from the bottom and lateral inlets of the lower chamber (Figure 1B, top). The semi-conical shape of this chamber was designed to enable the post wash gas phase volume reduction of the cell suspension: this shape stabilizes an injected air bubble which occupied the top part of the bottom chamber, leaving behind a volume reduced cell suspension (Figure 1B, middle) that was collected directly into a syringe (Figure 1B, bottom); these process steps are shown in the supplementary movies S1-3 (A with dye and B with cells) and S4. The fixed process inputs and parameters are listed in Table I; the operating temperature was kept at 21 ± 2°C.

2.3. Cell counts

The cell numbers and viability were counted using a Vi-CELL Cell Viability Analyser (Beckman Coulter, UK) before and after the cell suspension processing. The results are shown as percent viable

cell recovery (VCR) and correspond to the ratio between total viable cells after processing and total viable cells before processing.

2.4. DMSO measurement

The concentration of DMSO in the filtrate and retentate was measured by reverse phase high performance liquid chromatography (HPLC) using an Agilent 1200 series device (Agilent Technologies UK Limited) under the control of the Agilent Chemstation software. A 4 mm x 125 mm (internal diameter x length) Nucleosil C18 column with a particle size of 5 µm (Sigma-Aldrich, UK) was used as the stationary phase, while the mobile phase was based on a previously published protocol (Thumm et al. 1991). Briefly, an aliquot was taken from the filtrate or retentate sample and diluted 1:20 in 0.1% (v/v) Trifluoro Acetic Acid (TFA, Sigma-Aldrich UK). Calibration curves of CS 5 were prepared at the appropriate dilution and analyzed in parallel with the samples. The elution profile consisted of 100% distilled water in the first 5 min followed by a linear gradient of water/acetonitrile until 100% of acetonitrile was reached at 7 min; the reverse gradient was applied to reach 100% water at 9 min and maintained until 15 min. The DMSO peak was detected (210 nm detection wavelength) at 3-5 min of elution time. All results are presented as the ratio $\frac{C}{C_0}$, where C and C_0 are the final and initial concentration of DMSO, respectively.

2.5. FITC-Albumin experiments and quantification

To assess the removal of larger molecular weight molecules, 20 µL of conjugated Albumin-Fluorescein Isothiocyanate (FITC) (A9971, Sigma UK) at a concentration of 5 mg/mL in CS 5 were added to the 1 mL cell suspension immediately after thaw and before the filtration process. The Albumin-FITC concentrations were measured using a FluoStar Optima microplate reader (excitation 450 nm, emission 544 nm). Calibration curves of Albumin FITC in CS 5 were prepared at the appropriate dilution and analyzed in parallel with the samples. All results are presented as the ratio $\frac{C}{C_0}$, where C and C_0 are the final and initial concentrations of FITC-Albumin, respectively.

2.6. Pressure Measurements

The pressure in the lower chamber of the system was measured against the atmospheric pressure using either a manual or a digital manometer with data-logging capabilities (Sper Scientific, AZ US).

2.7. Filtration model

A modified form of the diafiltration equation was used to model and predict solute removal from the cell suspensions:

$$\frac{C}{C_0} = e^{-\frac{F \times t}{V_c} \times k} = e^{-N \times k} \qquad \text{Equation 1}$$

where F is the flow rate in mL/min, t is time in min, V_C is the lower (cell-containing) chamber volume, N is the number of diavolumes, defined as the quocient between the total volume used for filtration and the volume of the filtration chamber, and k is a wash efficiency parameter which is dependent on the geometry of the device.

2.8. Computational Fluid Dynamics

The commercial software package COMSOL Multiphysics 5.0 (Hatfield, Comsol, UK) was used to simulate the velocity, pressure and DMSO profiles in the filter device. The laminar flow application mode within the COMSOL Multiphysics software was chosen to simulate the velocity and pressure, whereas the mass transfer for diluted species application mode was chosen to simulate the DMSO profile. To lower the computer memory requirements of the overall simulation, the flow field is simulated first as the viscosity and densities of the culture medium containing DMSO are considered constant (relatively low species concentration). The solved flow field is then saved and coupled with a mass transfer model, which describes DMSO convection/diffusion in the filter device.

In all simulations, the boundaries of the filtering device were meshed with 52155 triangular elements (extra fine mesh; default settings) and its domain with 376906 quadrilateral elements (normal mesh option; default settings) using the free mesh option of COMSOL Multiphysics's mesh generator. The number of degrees of freedom was 377702. The convergence was tested by a two-fold increase in the number of elements. The velocity, pressure and DMSO concentration simulated by using the new mesh were agreed at the three significant figures level with the velocity, pressure and DMSO concentration simulated by using the default mesh. The simulation results are presented as contour plots, blue represents areas of low DMSO concentration and red represents areas of high values for DMSO concentration.

2.9. Flow Cytometry

The post filtration multipotency of the hMSCs was assessed using an hMSC phenotyping kit (Miltenyi Biotec, Surrey, UK) flow cytometry assay. Briefly, single cell suspensions, following wash and volume reduction using the novel filtration device, were equally divided into 7 samples. Antibodies were diluted 1:11 in 110ul buffer per 1x106 cells and incubated with the samples on ice for 30 minutes. The 7 samples for each MSC test consisted of 4 single fluorophore controls (CD105-PE, CD90-FITC, CD73-APC, CD14-/CD20-/CD34-/CD45-PerCP) for compensation, a cell only sample (incubated with 110ul FACS buffer, also for 30 minutes on ice), the Isotype Control Cocktail and the MSC Phenotyping Cocktail provided in the MSC phenotyping kit (Miltenyi). After antibody labelling, cells were washed and re-suspended in 0.5ml FACS buffer in flow analysis tubes (BD Bioscience, Oxford, UK). Flow cytometery was performed using a BD LSR II flow cytometer. For analysis, at least 50,000 events were initially gated based on forward and side scatter and forward scatter height against area was used for doublet removal. The isotype control cocktail was run with the same gating strategy and MSCs defined from gating the top 1% of isotype expression. To confirm an MSC phenotype, greater than 95% expression of CD105, CD90, CD73, and less than 2% expression of CD14, CD20, CD34 and CD45 must be observed (Dominici et al. 2006). N=3 samples were run and the standard deviation calculated.

2.10. Statistics

The statistical analysis was performed using the Excel data analysis add-on and the GraphPad software. The p-values presented were calculated for the two tails of the normal distribution and when more than 2 groups were compared Tukey's multicomparison test was used. The notation "n" (lowercase, not to be mistaken by uppercase "N", the diavolumes) was used to denote the number of independent replicates.

3. Results

To test this new filtration device it was necessary to choose a filter medium and a pore size which minimized the rate of pressure increase during the wash operation; initial tests demonstrated that a hydrophilic Polyvinylidene fluoride (hPVDF) with a nominal pore size of 0.65 μm was a feasible starting point (data not shown).

To maximize the number of cells recovered, it was hypothesized that a backflush step between the wash and concentration steps would dislodge cells from the filter membrane and increase the post process VCR. The wash step was performed using a flow rate of 2 mL/min via the bottom inlet and 5 mL/min through the lateral inlet (2/5 flow). While no significant difference in VCR was observed when this backflush step was present (compared to its absence), there were significant effects on the amount of solute removed. Figure 2A depicts the DMSO concentration in the filtrate over time, and it is visible that after the backflush step there is an increase in the DMSO concentration in the filtrate. It was hypothesized that the overall DMSO removal of the retentate could be enhanced if several backflush steps were applied during the wash phase. Figure 2B depicts the experimental design used to test this hypothesis, where 3 backflush steps were performed during a 2/5 wash for 10 min (3x backflush) and compared with a 10 min 2/5 wash with one backflush step after the wash operation (1x backflush). Figure 2C shows that the 3x backflush wash yielded a lower DMSO concentration than the 1x backflush wash, with 0.136 ± 0.003 and 0.20 ± 0.01 of the initial DMSO concentration, respectively ($n=3$, $p<0.001$). This increase in DMSO removal was also associated with a higher lower chamber pressure in the 3x backflush wash when compared with the 1x backflush wash, after 10 minutes, as shown in Figure 2D.

The individual contributions of the bottom and lateral flows for the DMSO removal from the cell suspension were investigated. Figure 3 shows that, after a 10 minutes wash period, the lateral flow reduces the initial amount of DMSO to 0.66 ± 0.09 ($n=5$) of its initial concentration. There was no significant difference between the concentration of DMSO after the bottom flow wash and the lateral+bottom (2/5) flow wash (0.25 ± 0.01, $n=3$ and 0.17 ± 0.06, $n=3$), for the 10 min wash period. However, the presence of a bottom flow results in a significantly higher DMSO reduction when compared to using lateral flow only ($p<0.01$).

The combinatorial effect of the lateral and bottom flows (2/5 flow) on DMSO reduction was further investigated as a function of the diavolumes *N* (Bottom Flow x Time), as shown in Figure 4A. The curve corresponding to the 2/5 flow is in agreement with the diafiltration equation, with the wash efficiency value ***k*** being constant ($R^2=0.998$); without the lateral flow, the bottom flow curve deviates from Equation 1, yielding lower DMSO reduction values. These differences correlate with different

pressure profiles (Figure 4B): the lateral flow of PBS leads to an increased pressure ending in 80 mbar, whereas pressure in the bottom flow configuration is kept at 20 mbar or less.

To be useful as part of a point of care device, this filter will be manufactured as an injection molded part, like most medical devices or bioprocessing consumables. The panels C and D in Figure 4 depict a PMMA filter device which houses an injection molded (IM) COC lower chamber whose shape is identical to the one in Figure 1A. This IM device was used to process thawed MRC-5 cell suspensions at 2 mL/min bottom flow, without lateral flow, for 24 min and the volumes, cell concentration and DMSO removal are shown in Table 2. The DMSO reduction for this data was 91 ± 2% for N=32, as shown in Figure 4A. The cell recovery and volume reduction was 84 ± 1% and 2.7 ± 0.5 fold, respectively. These results demonstrate that this filtration system can be successfully used for small volume cell suspension wash and volume reduction, with a cell recovery of more than 80%. Moreover, the use of a thermoplastic material indicates that the performance of the PMMA device is close to the performance of the consumable.

The filtration device was redesigned to increase the DMSO reduction while avoiding pressure build-up in the lower chamber, i.e. increasing the wash without using the lateral flow. Figure 5A shows the 3 geometries of the filtration device, where M1 (mark 1) is the original design, with a lower chamber height (bottom inlet to filter membrane) of 0.8 cm and a filtration area of 3.5 cm^2. To minimize the diffusional distances and increase the fluid velocity, the M2 geometry was designed to increase the height of the chamber by 50% (compared to M1) while maintaining a constant volume, thus decreasing the cross sectional area of the bottom flow chamber. This was achieved by changing the chamber from a round bottom to a V-bottom shape. Computational fluid dynamics (CFD) was used to model DMSO removal in M2 under the 2/5 flow configuration; the surface plot in figure 5B depicts the top view of the M2 device and it indicates that there is accumulation of DMSO in the outer area of the membrane. Again, these areas are the furthest away from the bottom flow jet and they could be designed out (or "trimmed" out) of the M2 geometry thus yielding the M3 geometry, with a 2.5 cm^2 area (30% decrease vs M2) and a lower chamber height of 1.5 cm (25% increase vs M2). These geometry changes had significant effects on the DMSO removal rate, as demonstrated in Figure 5C. When using only the bottom inlet to flow wash buffer through the cell suspension (solid lines) it is

visible that the amount of DMSO removed per diavolumes of buffer increases from M1 to M3. Unlike the M1 and M2 bottom flow curves, the M3 curve fits a single exponential line as described in Equation 1 (solid line, R^2=0.97); likewise, when the lateral flow is used for the M1 and M2 geometries, their DMSO reduction curves also fit a single exponential decay (solid lines, R^2=0.97 for both). However, the M3 geometry, operating with bottom flow only, sustains the lower chamber pressure below 15 mbar, whereas the M1 and M2 geometries, operating with the 2/5 flow, can reach pressures of 100 and 400 mbar, respectively (Figure 5D, n=3). These data indicate that the M3 geometry enables an efficient DMSO reduction while operating at low pressures.

To further validate the hypothesis that the diffusional distance is the critical factor behind these increases in efficiency from M1 to M3, the differences in these geometries were factored into Equation 1. By keeping the volume of the chamber constant and increasing the height of the chamber, the whole shape becomes "thinner" along its length thereby reducing the diffusional distance and increasing the fluid velocity. As such, the increase in height is proportional to the increase in the amount of DMSO removed. To incorporate this into equation 1 it should be noted that the effect of the height implies that for the same level of DMSO removal, less diavolumes (N) are needed as the height is increased. In this way, N should be replaced by the product N×height. However, since this is an exponential term it must be dimensionless. Since N is dimensionless so should the height be; to achieve this it was noted that height=sin(α)×longer slope (as per figure 5E) and the sin(α) was used instead of the height. Thus, Equation 1 can be modified to:

$$\frac{C}{C_0} = e^{-\frac{Ft}{V_c}k\sin\alpha} = e^{-Nk\sin\alpha} \qquad \text{Equation 2}$$

The semi-logarithmic plot of $\frac{C}{C_0}$ vs $N \times \sin\alpha$ is depicted in Figure 5F. This plot shows that the data points derived from Equation 1 in Figure 5C (M1 and M2 with lateral flow and M3 with bottom flow) can be modelled by a single curve using Equation 2 (R^2=0.98).

The M3 geometry was further characterized by its ability to reduce the amount of a model protein, albumin-FITC; After a 32 diavolumes wash the initial concentration of this protein was reduced by 94 ± 1% (Figure 5G). Furthermore, the viable cell recovery using M3 was 94 ± 5%, thus confirming that this geometry also enables a high cell recovery, while the volume reduction was 1.55 ± 0.08 fold

(Table 2). To assess the functionality and long-term viability of the cells after being processed, the M3 geometry was manufactured in stainless steel 316. Figure 5H demonstrates that, after a 16 diavolumes wash, the MRC-5 cell line still grows at the same specific rate as fresh cells or cells which have also been thawed but processed using a bench top centrifuge (see methods). Importantly, cell counts after a 24 hour culture showed that after thawing, processing and plating 62 ± 15% of the cells (post thaw counts) survived; when no cell processing was performed and cells were directly plated in adherent flasks, the cell recovery was 58 ± 5% (n=4).

To validate this geometry for cell therapy applications, hMSCs were processed using the M3 geometry filtration device. The post filtration characterization of these cells was performed according to the ISCT criteria (Dominici et al. 2006) and the 3 cell runs (generated from 2 donors) showed that hMSCs retained their characteristic surface markers (Figure 6 A and B), while retaining their ability to adhere to plastic, proliferate (Figure 6E and F) and the capability for chondrogenic, osteogenic and adipogenic differentiation (Figure 6G, H and I). The viable cell recovery after these 3 runs ranged from 73 to 99%, while the DMSO removal ranged from 86-88% (Figure 6 C and D).

4. Discussion

In this work, we have designed and characterized a filtration system to process thawed cell suspensions which removes more than 90% of the DMSO and recovers more than 80% of the viable cells. Most importantly, this filtration system does not require an outside loop like a TFF system, thus minimizing the shear stress that cells are exposed to and the area where liquid can be lost by adsorption.

The central element of the filter housing design (Figure 1A) is the laminar flow that is established at these dimensions and flow velocities. While it is visible that the cell suspension has settled at the end of the filtration process, it is unlikely that cell settling can be faster than the flow rate of wash buffer from the bottom inlet. The average linear velocity of wash buffer crossing the membrane from the bottom flow is 0.57 cm/min while the average cell settling velocity is at least one order of magnitude below this velocity (Chalmers et al. 1999). Another possibility is that the settling velocity of the cells is increased in the Cryostor media; while this is true in absolute terms, because the CS5 is hypertonic,

it is the density difference between the cells in CS5 and the CS5 medium that is relevant for the settling velocity. Thus, it is expected that the density differences between fresh cells in PBS and thawed cells in CS5 are the same; this was confirmed by an isopycnic centrifugation using a Percoll gradient (Supplementary Figure 1) which confirmed that the density of the MRC-5 cells in CS5 is between 1.04 and 1.06 g/mL, whereas the literature reports a similar density for these cells in PBS (1.05 g/mL) (Birnie and Rickwood 1980).

Using the lateral flow configuration, the DMSO concentration was reduced to 0.66 of its initial value (Figure 4); interestingly, this value is the same as the ratio of the cell suspension volume to the lower chamber volume (1mL/1.5mL), which strongly suggests that the lateral flow alone does not remove any significant amount of DMSO after 10 minutes. Nevertheless, the addition of lateral flow to the bottom flow (2/5 flow) seems to provide a more efficient mixing for both M1 and M2 geometries, and thus a better reduction in DMSO concentration, when compared with using the bottom flow only (Figure 5C). These results follow the same trend as the use of increased backflush cycles to enhance DMSO reduction (Figure 2), also at the expense of higher pressure differences. Taken together, these two data sets strongly suggest that both the lateral flow and the backflush cycles increase the DMSO removal, by dispersing the cell bed that is established if bottom flow only is used. The design changes that lead to the M3 geometry had the goal of avoiding the dispersion of the cell bed that results in increased lower chamber pressures This was accomplished by prioritizing the minimization of the average diffusional length and the maximization of the fluid velocity. The M3 geometry, while having a lower volume reduction capability when compared to M1, does not require lateral flow to have a single exponential wash profile, as described by equation 1, while washing more than 95% of the DMSO using less diavolumes; using only one inlet to flow the wash buffer makes the operation simpler and will decrease the manufacturing cost of the POC device. The empirical model described by Equation 2 validates the aforementioned design hypothesis, as depicted in Figure 5F; when the DMSO removal curve fits equation 1, the different geometries can be normalized to the distance between the filter membrane and the bottom flow inlet. Both the M1 and M2 geometries DMSO removal data points shift to the right of the curve in Figure 5F when only bottom flow is used, a result which can be explained by cell settling in a low shear environment. The M3 filtration device was also

shown to remove up to 94% of a model protein, Albumin-FITC (Figure 5 G); this ability to removes higher molecular weight contaminants from cell suspensions can be of high value when the whole cell therapy process is considered.

The processing of hMSCs (Figure 6) demonstrated the capability of this novel filtration device for small volume cell wash, using cells relevant for cell therapy. Despite the DMSO removal efficiency being lower than for the MRC-5 cells wash, 88% of the DMSO was removed from hMSC cell suspensions. This lower washing efficiency can be attributed to different biophysical characteristics, namely cell size, and it is a clear area of research in the development of this technology. Another point for future research is how to have sterility as a release criterion for the cellular therapies, since this takes about 24h to be tested and the therapies need to be administered within minutes.

In a broader sense, a simple solid-liquid separation device for small volumes is a key enabling technology to make the distributed manufacturing of cellular therapies possible.

Acknowledgments

The authors thank John Vincent, Sarah Callens (eXmoor Pharma, UK), Jesus Zurdo (Lonza UK) and Behzad Mahdavi (Lonza Walkersville, US) for the valuable technical discussions, John Langlon and Erich Herrmann (UCL Department of Biochemical engineering workshop) for the useful discussions and device machining.

This work was supported by Innovate UK, under the collaborative R&D project CPREP and by the Department of Biochemical Engineering, University College London, UK. The CPREP project was a collaboration between Lonza UK, UCL, Amercare Ltd and eXmoor Ltd and the resulting technology has been licensed to Closed Cell Systems Ltd (CCS) (Supplementary Figure 2 shows the processor and consumable which use this filtration device for the solid-liquid separation).

Competing financial interests

RT and FV are authors and have financial interests in 2 patents related to this work, which were licensed to CCS. None of the manuscript's authors have any other financial interest in the company CCS. The authors have no other competing financial interests.

5. Bibliography

Abdelkefi A, Lakhal A, Moojat N, Hamed LB, Fekih J, Ladeb S, Torjman L, Othman TB. 2009. Severe neurotoxicity associated with dimethyl sulphoxide following PBSCT. Bone Marrow Transplant. England. p 323-4.

Birnie G, Rickwood D. 1980. Centrifugal Separations in Molecular and Cell Biology. Journal of Basic Microbiology 20(2):153.

Chalmers JJ, Haam S, Zhao Y, McCloskey K, Moore L, Zborowski M, Williams PS. 1999. Quantification of cellular properties from external fields and resulting induced velocity: cellular hydrodynamic diameter. Biotechnol Bioeng 64(5):509-18.

Cox MA, Kastrup J, Hrubisko M. 2012. Historical perspectives and the future of adverse reactions associated with haemopoietic stem cells cryopreserved with dimethyl sulfoxide. Cell Tissue Bank 13(2):203-15.

Dominici M, Le Blanc K, Mueller I, Slaper-Cortenbach I, Marini F, Krause D, Deans R, Keating A, Prockop D, Horwitz E. 2006. Minimal criteria for defining multipotent mesenchymal stromal cells. The International Society for Cellular Therapy position statement. Cytotherapy 8(4):315-7.

FDA. 1997. Food and Drug Administration Guidance for Industry - Q3C Impurities: Residual Solvents.

Galvao J, Davis B, Tilley M, Normando E, Duchen MR, Cordeiro MF. 2014. Unexpected low-dose toxicity of the universal solvent DMSO. Faseb j 28(3):1317-30.

Hanna J, Hubel A, Lemke E. 2012. Diffusion-based extraction of DMSO from a cell suspension in a three stream, vertical microchannel. Biotechnol Bioeng 109(9):2316-24.

Jaouen P, Vandanjon L, Quéméneur F. 1999. The shear stress of microalgal cell suspensions (Tetraselmis suecica) in tangential flow filtration systems: the role of pumps. 68(2):149–154.

Kuo JS, Zhao Y, Schiro PG, Ng L, Lim DS, Shelby JP, Chiu DT. 2010. Deformability considerations in filtration of biological cells. Lab Chip 10(7):837-42.

Mazur P. 1984. Freezing of living cells: mechanisms and implications. Am J Physiol 247(3 Pt 1):C125-42.

Rodríguez L, Azqueta C, Azzalin S, García J, Querol S. 2004. Washing of cord blood grafts after thawing: high cell recovery using an automated and closed system*. Vox Sanguinis 87(3):165-172.

Rowley S. 2009. Hematopoietic Stem Cell Cryopreservation: A Review of Current Techniques. Journal of Hematotherapy 1(3):233-250.

Rushton A, Ward A, Holdich R. 2000. Solid-liquid filtration and separation technology. New York: Wiley-VCH: Weinheim. 587 p.

Sánchez-Salinas A, Cabañas-Perianes V, Blanquer M, Majado M, Insausti C, Monserrat J, Sánchez-Ibáñez M, Menchón P, García-Hernández A, Gómez-Espuch J and others. 2012. An automatic wash method for dimethyl sulfoxide removal in autologous hematopoietic stem cell transplantation decreases the adverse effects related to infusion. Transfusion 52(11):2382-2386.

Tamagnini F, Scullion S, Brown JT, Randall AD. 2014. Low Concentrations of the Solvent Dimethyl Sulphoxide Alter Intrinsic Excitability Properties of Cortical and Hippocampal Pyramidal Cells. PLoS One.

Thumm W, Freitag D, Kettrup A. 1991. Determination and quantification of dimethyl sulphoxide by HPLC. Chromatographia 32(9):461-462.

Xu W, Chellam S. 2005. Initial Stages of Bacterial Fouling during Dead-End Microfiltration†. Environmental Science & Technology 39(17):6470-6476.

Zhou X, Liu Z, Shu Z, Ding W, Du P, Chung J, Liu C, Heimfeld S, Gao D. 2011. A dilution-filtration system for removing cryoprotective agents. J Biomech Eng 133(2):021007.

Table Legends

Table 1 – Fixed inputs and parameters for the operation of the filtration device.

Table 2 – Viable cell recovery, volume reduction and cell suspension viability after the filtration operation, under 2mL/min bottom flow for 24 minutes, without lateral flow, for the injection molded version of the filtration device.

Table 3 – Viable cell recovery, volume reduction and cell suspension viability using the M3 geometry, under 2 mL/min bottom flow for 24 min, without lateral flow.

Figure Legends

Figure 1 – Filtration device design and fluid flow. A)- CAD drawing of the filtration device housing, divided in a top and bottom part (A, top); when the device is assembled (A, bottom) the filter is located between the two parts and the cell suspension is introduced into the bottom, where it is washed, concentrated and loaded into a syringe (B, Supplementary videos). Panel C) depicts the fluid flow in the device: for visualization purposes, a red dyed PBS solution was used to wash 1 mL of a (transparent) cell-free CryoStor5 solution (the full video is available in Supplementary Video S2A). This frame corresponds to t=1s in the wash process.

Figure 2 – DMSO removal is enhanced by backflush frequency. The filter device was operated for 10 min in the wash mode with a 2 mL/min bottom flow rate and a 5 mL/min cross flow rate; after this wash step and before the concentration step a backflush was performed to dislodge cells from the filter membrane (see methods). The concentration of DMSO in the collected filtrate fractions increases after backflush (A). The backflush step was repeated 3 times throughout the wash period (3xbackflush) and compared to a single backflush after the wash step (1xbackflush) (B) for the amount of DMSO left in the cell suspension (lower chamber, which contains the retentate) (C) and the pressure difference generated in the lower chamber (D). ***, $p<0.001$.

Figure 3 – Lateral flow wash alone shows a limited DMSO reduction. The filter device was operated for 10 minutes in the wash mode with a 2 mL/min bottom flow rate without cross flow (20 mL, n=3), with a 5 mL/min lateral flow rate without bottom flow (Lateral 5 mL/min, n=3) and with a 2 mL/min bottom flow rate and a 5 mL/min cross flow rate (2/5 flow, n=6). ***, $p<0.001$ (Tukey's multicomparison test).

Figure 4 – Synergistic effect of the lateral and bottom flows. The presence of lateral flow during cell washing yields a DMSO reduction profile described by a single exponential function, as predicted by equation 1 (A, closed squares, $n\geq3$ for all data points), whereas in the absence of the lateral flow, the bottom flow wash does not fit the equation 1 model (A, closed circles, $n\geq3$ for all data points). The typical pressure profiles for these 2 wash modes show that the presence of cross flow also leads to pressure build-up in the lower chamber, unlike the bottom flow only operation mode (B). To mimic

the final thermoplastic product the bottom flow chamber geometry was injection molded (C, purple) to fit a PMMA housing (C, gray).

Figure 5 – Redesigning the filtration device for improved DMSO removal. The original filtration device was redesigned by changing the geometry of the bottom chamber which holds the cell suspension, which led to changes in the distance between the bottom inlet and the filter membrane, and filtration area (A). A CFD analysis on the M2 geometry revealed "dead zones" where the DMSO was being removed with less efficiency (B). The 3 different geometries were evaluated for their DMSO reduction capability (C, $n \geq 3$ for all data points), operated with (open symbols) and without (closed symbols) lateral flow, except for M3, where lateral flow lead to clogging (data not shown); the final pressure in the lower chamber, after 24 min, also revealed differences between geometries and wash modes (D, n=3 for all data points). The sine of the angle α, formed between the horizontal plane and the lower chamber slope that connects the bottom and lateral inlets (E), is different between devices; when the number of diavolumes is multiplied by the $\sin(\alpha)$, specific for each device, the curves that obey equation1 in C follow a single exponential decay empirical model, as described by equation 2 (F). The M3 geometry was assessed for its ability to reduce albumin-FITC by washing a cell suspension for 24 minutes at 2mL/min bottom flow (G); furthermore, the cellular proliferation after filtration processing, using the M3 geometry (n=4), was compared with post-centrifugation processing (n=5) and fresh cell culture processing (i.e. cell counts during passaging, n=5) by calculating the specific growth rate μ (day^{-1}).

Figure 6 – hMSC post filtration recovery, proliferation and characterization**.** hMSCs were processed using the M3 geometry filtration device. The post filtration characterization after 3 cell runs (generated from 2 donors) was performed according to the ISCT criteria: cell surface markers (Figure 6 A, individual flow cytometry histograms, and B, aggregate results from the 3 cell runs), adherence to plastic (Figure 6E, scale bar=400 mm) and the capability for chondrogenic, osteogenic and adipogenic differentiation (Figure 6G, H, scale bar=100 mm, and I, scale bar=50 mm, respectively). The viable cell recovery, DMSO removal and hMSC growth rates after filtration are displayed in Figure 6 C, D and F, respectively).

Supplementary Figure 1 – Isopycnic gradient centrifugation of MRC-5 cells in CryoStor 5. A cell suspension of 10^7 MRC-5 cells and a set of density marker beads (Cospherix, CA, USA) were centrifuged in parallel in a 5-layer CS5/Percoll (GE Healthcare) gradient. This gradient was established by overlaying CS5/Percoll solutions, in two 50 mL tubes, at a decreasing concentration of Percoll (50, 40, 30, 20 and 10%); after overlaying the cell or marker bead CS5 suspension, the two tubes were centrifuged at 4ºC for 30 min without acceleration or brake.

Supplementary Figure 2 – Processor with the docked consumable (left) and the consumable only (right) for the commercial version of the CPrep device. The frozen cellular therapy is delivered from a centralized manufacturing facility to the hospital. When a patient is ready the frozen vial is placed into the CPREP consumable (yellow area), which is already docked to the processor. Here it is thawed before being pumped into the novel filter device where the DMSO is washed out. After the washing step the cells are drained into a syringe ready for administration. This entire fluidic circuit is an integral part of the consumable.

Supplementary Video S1A and S1B – Loading using the novel filtration device. Video of the loading process for CS5 with Alizarin Red (Supplementary Video 1A) and 10^7 MRC-5 cells (Supplementary Video 1B).

Supplementary Video S2A and S2B – Washing using the novel filtration device. Video of the washing process for PBS with Alizarin Red (Supplementary Video 2A, the dye has been dissolved in PBS to visualize the jet flow from the bottom inlet to the membrane) and 10^7 MRC-5 cells (Supplementary Video 2B).

Supplementary Video S3A and S3B – Backflush using the novel filtration device. Video of the backflush process for CS5 with Alizarin Red (Supplementary Video 3A) and 10^7 MRC-5 cells (Supplementary Video 3B).

Supplementary Video S4 – Volume reduction using the novel filtration device. Video of the volume reduction process for CS5 containing 10^7 MRC-5 cells.

Table 1

Parameter/input	Value
Cell type	MRC-5 (lung fibroblast cell line)
Wash buffer	Phosphate buffered saline (PBS)
Cryopreservation solution	CryoStor-5 (5% DMSO)
Initial cell suspension volume	1 mL
Initial cell suspension concentration	10^7/mL
Cell chamber volume	1.5 mL
Total process time (w/o priming or manual steps)	≤ 30min
Cell loading flow rate	2 mL/min
Lateral flow rate	5 mL/min
Backflush flow rate and time	5 mL/min for 10 sec (between wash and concentration)
Air flow rate (volume reduction)	1 mL/min

Fixed inputs and parameters for the operation of the filtration device.
254x190mm (96 x 96 DPI)

Table 2

Run #	V_in (mL)	V_out (mL)	pre-process viable cell concentration (10^6/mL)	Input viability (%)	post-process viable cell concentration (10^6/mL)	Output viability (%)	Fold volume reduction	Total viable cell recovery (%)
1	1.086	0.393	15.5	89	56.1	92	2.8	84
2	0.821	0.408	12.1	88	20.1	91	2	83
3	1.052	0.334	10.8	91	28.8	94	3.1	85
4	0.952	0.322	10.9	88	27.5	92	3	85
Average	**1.0**	**0.36**	**12**	**89**	**28**	**92**	**2.7**	**84**
stdev	0.1	0.04	2	1	7	1	0.5	1
rel stdev (%)	10	11	17	1	25	1	19	1

Viable cell recovery, volume reduction and cell suspension viability after the filtration operation, under 2mL/min bottom flow for 24 minutes, without lateral flow, for the injection molded version of the filtration device.
254x190mm (96 x 96 DPI)

Table 3

M3 Run #	V_in (mL)	V_out (mL)	pre-process viable cell concentration (10^6/mL)	Input viability (%)	post-process viable cell concentration (10^6/mL)	Output viability (%)	Fold volume reduction	Total viable cell recovery (%)
1	1.03	0.68	9.7	70.2	13.6	89.1	1.52	92
2	1.00	0.66	10.2	86.6	14.1	89.1	1.52	91
3	0.96	0.65	10.2	89.0	15.7	89.0	1.49	103
4	1.04	0.62	9.3	83.4	14.1	85.9	1.69	89
5	0.92	0.61	8.8	89.5	12.4	87.8	1.51	93
Average	1.01	0.65	10	84	14	88	1.55	94
Std. dev.	0.04	0.03	1	8	1	1	0.08	5
C.V.(%)	4	5	10	10	7	1	5	5

Viable cell recovery, volume reduction and cell suspension viability using the M3 geometry, under 2 mL/min bottom flow for 24 min, without lateral flow.
254x190mm (96 x 96 DPI)

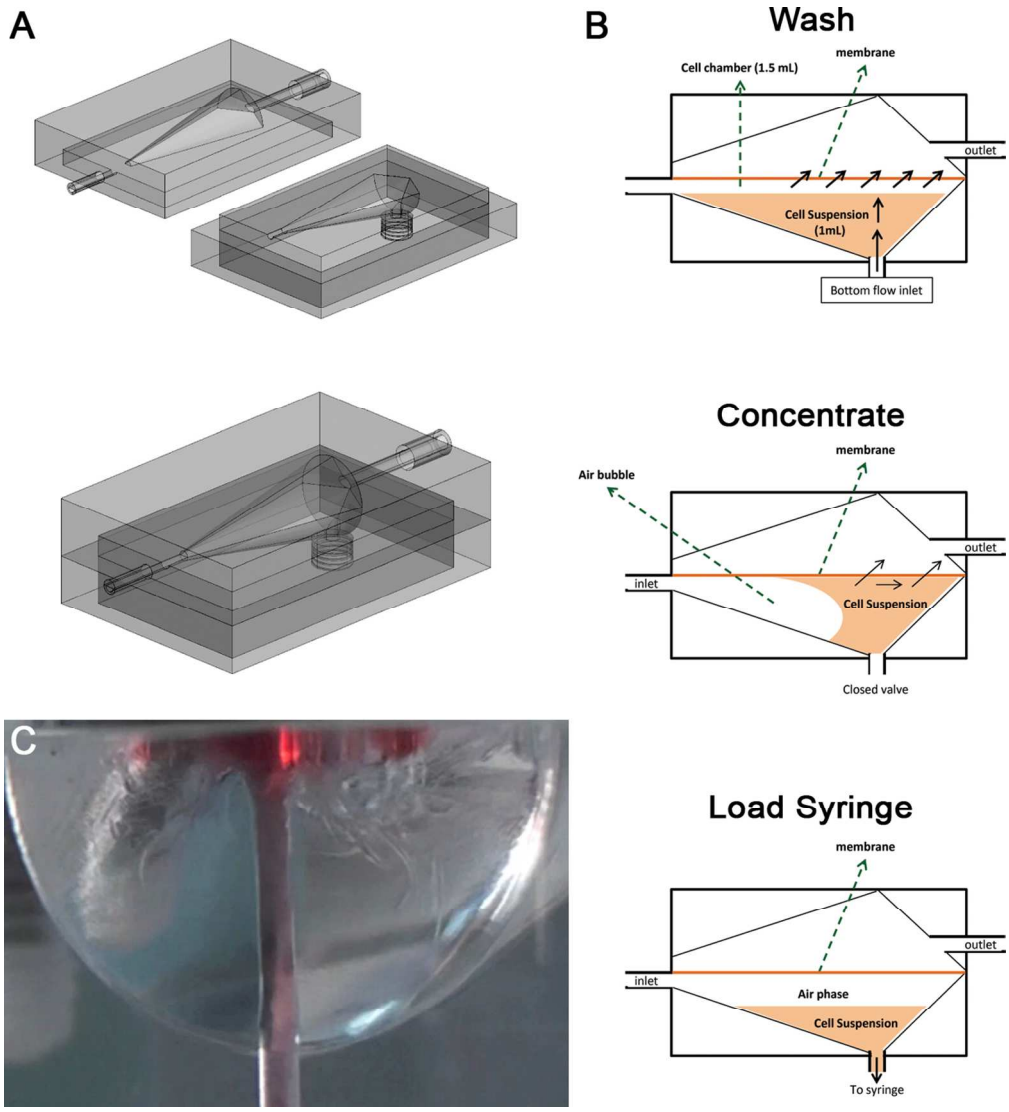

Filtration device design and fluid flow. A)- CAD drawing of the filtration device housing, divided in a top and bottom part (A, top); when the device is assembled (A, bottom) the filter is located between the two parts and the cell suspension is introduced into the bottom, where it is washed, concentrated and loaded into a syringe (B, Supplementary videos). Panel C) depicts the fluid flow in the device: for visualization purposes, a red dyed PBS solution was used to wash 1 mL of a (transparent) cell-free CryoStor5 solution (the full video is available in Supplementary Video S2A). This frame corresponds to t=1s in the wash process.
115x127mm (300 x 300 DPI)

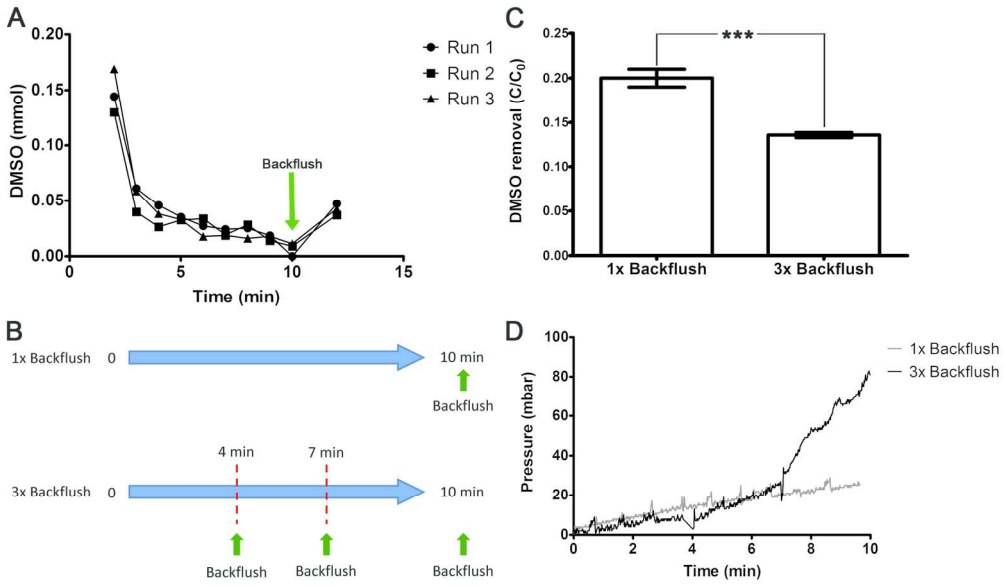

DMSO removal is enhanced by backflush frequency. The filter device was operated for 10 min in the wash mode with a 2 mL/min bottom flow rate and a 5 mL/min cross flow rate; after this wash step and before the concentration step a backflush was performed to dislodge cells from the filter membrane (see methods). The concentration of DMSO in the collected filtrate fractions increases after backflush (A). The backflush step was repeated 3 times throughout the wash period (3xbackflush) and compared to a single backflush after the wash step (1xbackflush) (B) for the amount of DMSO left in the cell suspension (lower chamber, which contains the retentate) (C) and the pressure difference generated in the lower chamber (D). ***, $p<0.001$.
160x94mm (300 x 300 DPI)

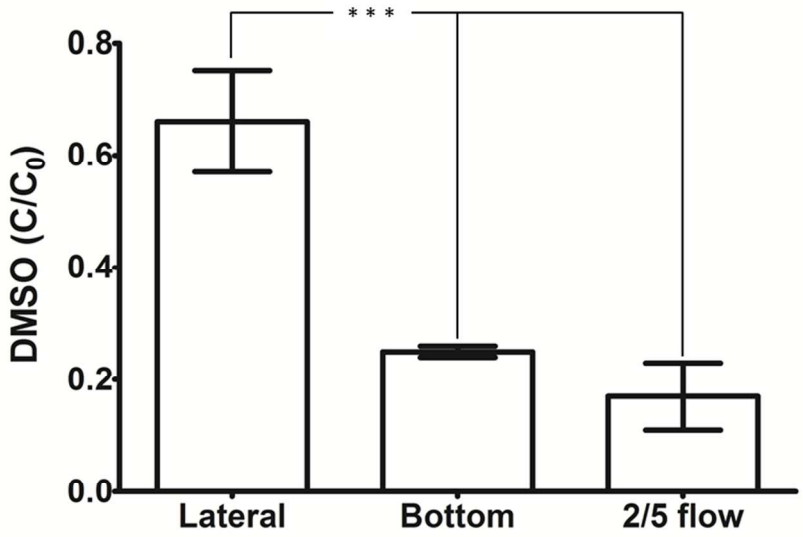

Lateral flow wash alone shows a limited DMSO reduction. The filter device was operated for 10 minutes in the wash mode with a 2 mL/min bottom flow rate without cross flow (20 mL, n=3), with a 5 mL/min lateral flow rate without bottom flow (Lateral 5 mL/min, n=3) and with a 2 mL/min bottom flow rate and a 5 mL/min cross flow rate (2/5 flow, n=6). ***, p<0.001 (Tukey's multicomparison test).
254x190mm (96 x 96 DPI)

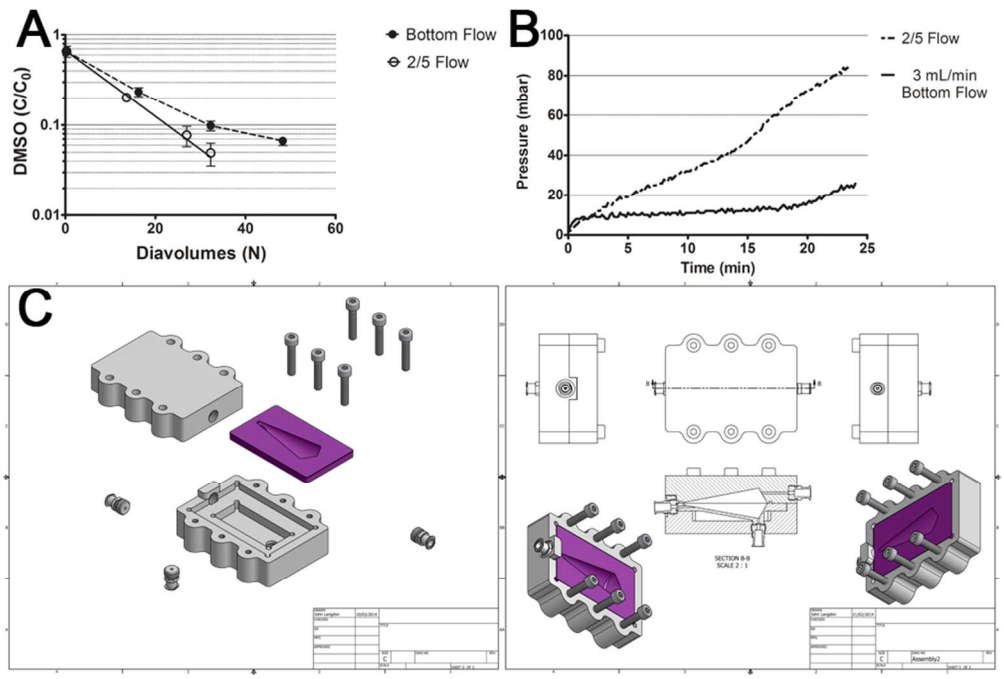

Synergistic effect of the lateral and bottom flows. The presence of lateral flow during cell washing yields a DMSO reduction profile described by a single exponential function, as predicted by equation 1 (A, closed squares, n≥3 for all data points), whereas in the absence of the lateral flow, the bottom flow wash does not fit the equation 1 model (A, closed circles, n≥3 for all data points). The typical pressure profiles for these 2 wash modes show that the presence of cross flow also leads to pressure build-up in the lower chamber, unlike the bottom flow only operation mode (B). To mimic the final thermoplastic product the bottom flow chamber geometry was injection molded (C, purple) to fit a PMMA housing (C, gray).
85x56mm (300 x 300 DPI)

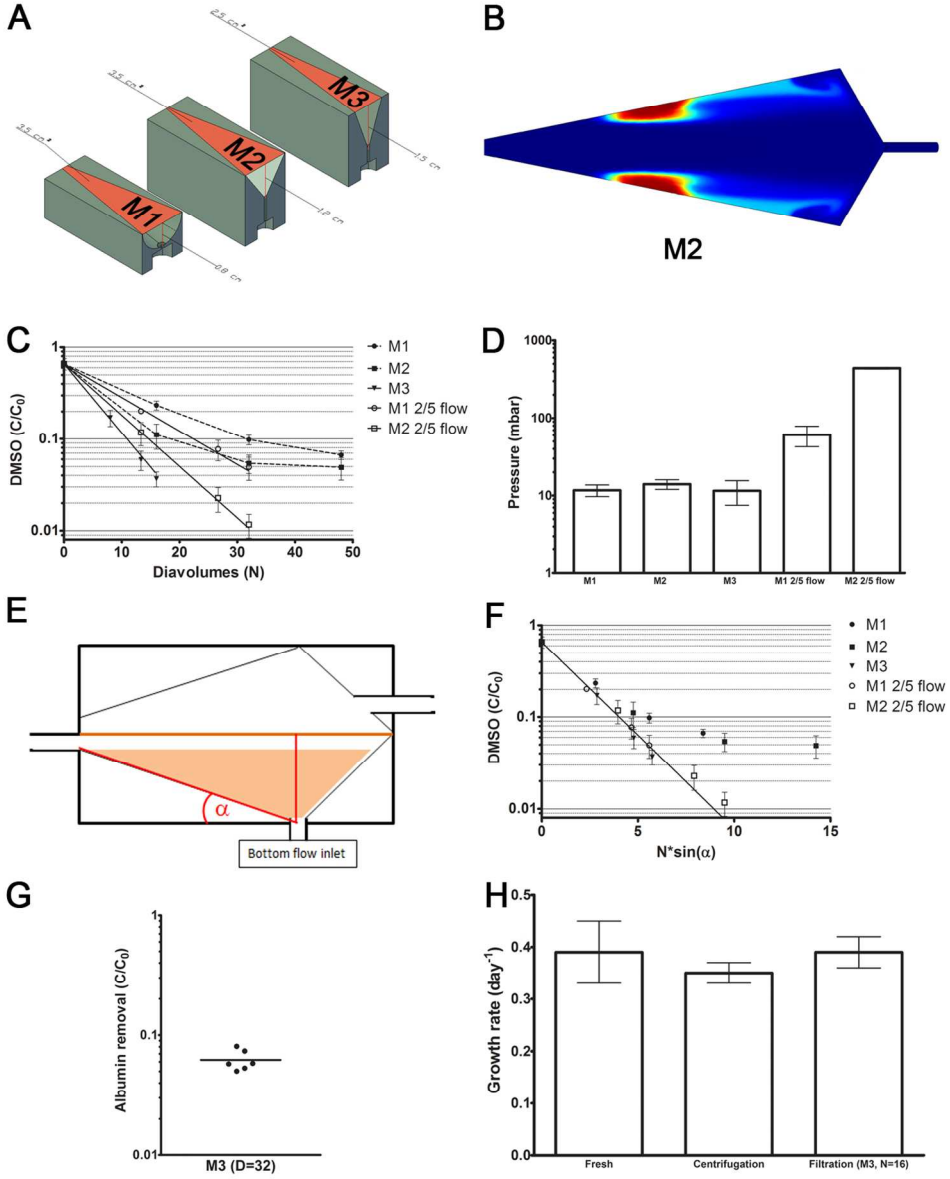

– Redesigning the filtration device for improved DMSO removal. The original filtration device was redesigned by changing the geometry of the bottom chamber which holds the cell suspension, which led to changes in the distance between the bottom inlet and the filter membrane, and filtration area (A). A CFD analysis on the M2 geometry revealed "dead zones" where the DMSO was being removed with less efficiency (B). The 3 different geometries were evaluated for their DMSO reduction capability (C, n≥3 for all data points), operated with (open symbols) and without (closed symbols) lateral flow, except for M3, where lateral flow lead to clogging (data not shown); the final pressure in the lower chamber, after 24 min, also revealed differences between geometries and wash modes (D, n=3 for all data points). The sine of the angle α, formed between the horizontal plane and the lower chamber slope that connects the bottom and lateral inlets (E), is different between devices; when the number of diavolumes is multiplied by the sin(α), specific for each device, the curves that obey equation1 in C follow a single exponential decay empirical model, as described by equation 2 (F). The M3 geometry was assessed for its ability to reduce albumin-FITC by washing a cell suspension for 24 minutes at 2mL/min bottom flow (G); furthermore, the cellular proliferation

after filtration processing, using the M3 geometry (n=4), was compared with post-centrifugation processing (n=5) and fresh cell culture processing (i.e. cell counts during passaging, n=5) by calculating the specific growth rate μ (day-1).
119x150mm (300 x 300 DPI)

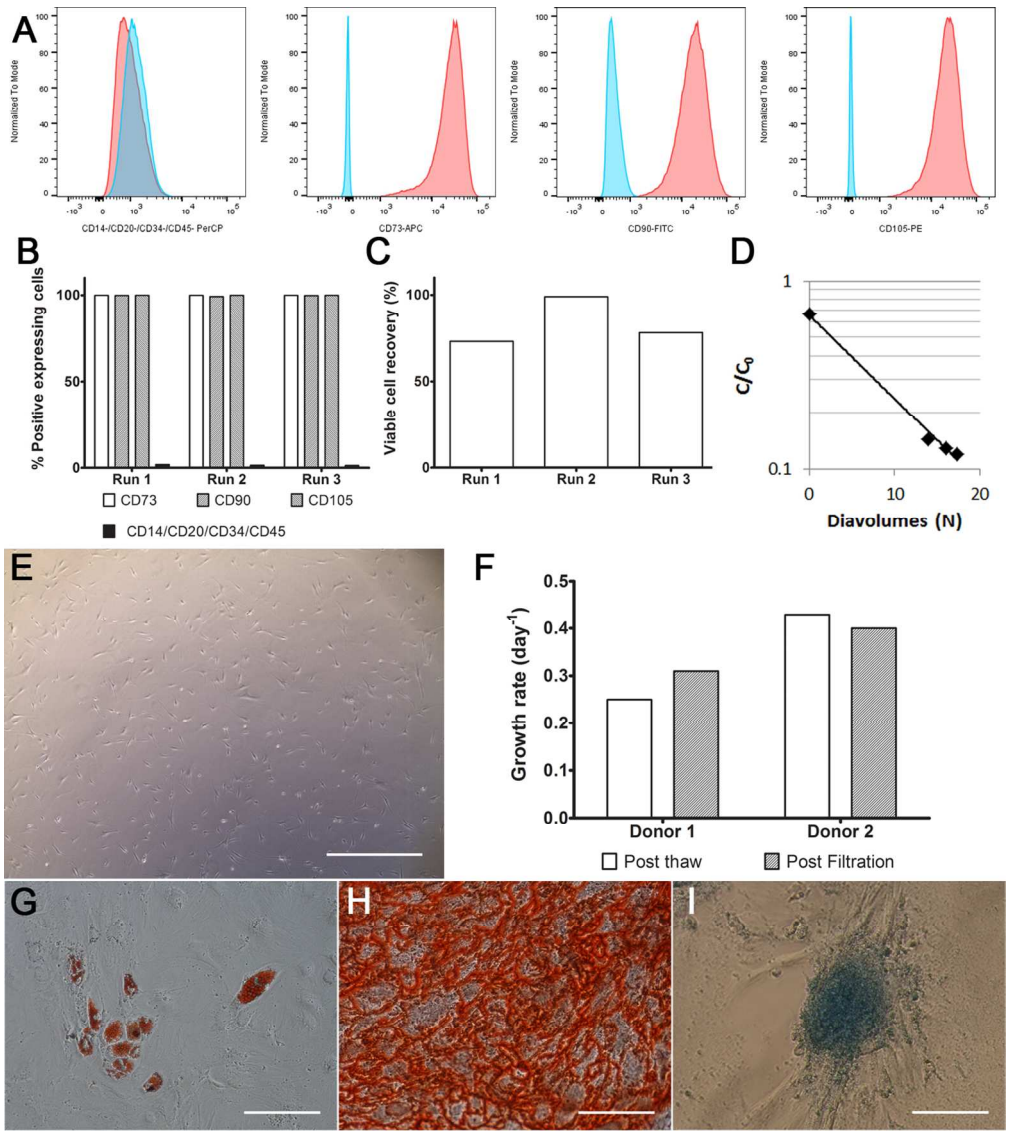

hMSC post filtration recovery, proliferation and characterization. hMSCs were processed using the M3 geometry filtration device. The post filtration characterization after 3 cell runs (generated from 2 donors) was performed according to the ISCT criteria: cell surface markers (Figure 6 A, individual flow cytometry histograms, and B, aggregate results from the 3 cell runs), adherence to plastic (Figure 6E, scale bar=400 µm) and the capability for chondrogenic, osteogenic and adipogenic differentiation (Figure 6G, H, scale bar=100 µm, and I, scale bar=50 µm, respectively). The viable cell recovery, DMSO removal and hMSC growth rates after filtration are displayed in Figure 6 C, D and F, respectively).
119x134mm (300 x 300 DPI)